Transactions of the TSME (2017) Vol. 5, No. 1, 4-19
Journal of Research and Applications in Mechanical Engineering

ISSN 2229-2152 print
DOI:

Research Article

NUMERICAL SIMULATION OF BULK MATERIALS OF ENERGY DISSIPATION IN DUSTINESS TESTERS USING DEM

S. Wangchai[1,*]
D.B. Hastie[2]
P.W. Wypych[2]
[1] Department of Materials Handling & Logistics Engineering, Faculty of Engineering, King Mongkut's University of Technology North Bangkok, 10800, Thailand
[2] School of Mechanical, Materials, Mechatronic and Biomedical Engineering, Faculty of Engineering and Information Sciences, University of Wollongong, NSW 2522, Australia

ABSTRACT:
Dust generation occurs in many bulk material handling processes, including; during free fall, transport hubs of handling of bulk materials, granular material loading or unloading and impact on conveyor transfers or other materials. Dust can pose an air pollution problem in; communities, the environment, industry equipment and be hazardous to health. Dustiness testers are one method that can be used to measure the amount of dust generation. It is known that the energy will need to remove the mass of material from the surface at the particle impact condition, particle velocity, particle collision and particle size distribution. However, it is often difficult to calculate the amount of energy absorbed on the surface. This paper investigates the energy dissipation phenomenon of two materials, iron ore and coal with size range 2.0-6.3 mm diameter. The discrete element modelling (DEM) simulation of the material movement in the European Standard dustiness tester and the Australian Standard dustiness tester have been used to analyse the collision energy and frequency, energy dissipation of bulk materials flow. Therefore, the DEM method was developed to simulate the energy dissipated of bulk materials during impact in the dustiness testers with these techniques and details of the modelling are presented in this paper.

Keywords: *Discrete element method (DEM), Dustiness tester, Impact energy, Energy dissipation, Particle size distribution, Bulk Materials*

1. INTRODUCTION

The handling, transportation and loading and/or unloading of bulk materials all have the potential to generate dust. The formation and emission of dust during handling depends on the type of material handling, size distribution of generated particles, and properties of the material [1-3]. Dust emissions are creating an increasing number of problems in industry, health effects on workers, environmental pollution and leading to the defective condition of products in manufacturing processes and parts of machinery [4, 5]. Dustiness of a material is defined as the propensity of a material to emit dust during handling and a measure of the dustiness of a material can be obtained from dustiness testing (rotating drum methods) [6]. There are two standards for dustiness testing used for powder or granular materials in rotating drum testers such as the European standard dustiness tester [7] and the Australian standard dustiness tester [8], both standards are used to measure the dustiness of bulk materials.

The Discrete Element Method (DEM) is becoming an increasingly popular method for simulation analysis and visualisation of the materials flow and impact on other particles or the wall of the drum. The principle of DEM is to track in a time stepping simulation, the rotation and trajectory of each particle in the drum to evaluate the position

* Corresponding author: S. Wangchai
E-mail address: sathaphon.w@eng.kmutnb.ac.th

and orientation of the particles and then to calculate the interactions between the particles themselves and also between the particles and their environment. Any particles broken to smaller particle size are a result of the particle impact stress being larger than the particle strength acting on the particles and were calculated based on Griffith's theory and Hertz's theory. Particle contact strength (σ_s) is determined by Griffith's theory[9]. Particle contact stress (σ_1) is the measure of particle impacts on the drum wall or the other particles. The mechanics of size reduction processes in a typical mode of breakage are presented, namely body breakage and surface breakage. Body breakage is a high-energy impact and surface breakage is a low energy impact. The importance of low energy impact and high energy impact events also contribute to particle breakage has been reported by Leung [10, 11]. The particle movement in the rotating drum is sliding and rolling that provide to the size distributions [12, 13].

This work extends the previous work of the authors [14] and presents a study of the application of DEM to simulate the material movement in the two standard dustiness testers [7, 8], which has been used to analyse the force structure in the dustiness tester and the impact energy of bulk materials flow. Particles having a spherical shape have been injected in the bottom of each rotating drum with the initial location being an even spread from the front to the back of the rotating drums. This paper also illustrates the DEM simulation of the particle-particle and particle-wall collision velocity, the particle collision energy and frequency in the normal and tangential directions and particle distribution in the radial velocity and axial velocity in the rotating drum with different particle sizes, contact stress and energy dissipation phenomenon of two materials, iron ore and coal with size range 2.0-6.3 mm diameter. Therefore, the DEM method was developed to simulate the energy dissipated of bulk materials during impact in the dustiness testers with these techniques and details of the modelling are presented in this paper.

2. EXPERIMENTAL SETUP

Iron ore and coal materials were chosen as the test material for investigation of the flow mechanisms of the particles within both dustiness testers. Table. 1 reports the three characteristics used in the selection of the two test materials because the purpose of the investigation was to visualise the particle flow in the rotating drums of the two dustiness testers, but not to measure the degree of dust generated as a result of the testing.

Table 1: Properties of iron ore and coal

Parameter/materials	Iron ore	Coal
Loose-poured bulk density (kg/m^3)	1475	697
Particle density (kg/m^3)	3867.8	1442.4
Particle size distribution (6.3 mm)	3.38%	13.2%
Particle size distribution (5.6 mm)	15.53%	26.4%
Particle size distribution (4.0 mm)	57.83%	49.7%
Particle size distribution (2.0 mm)	23.03%	10.7%

This is also vital for the DEM simulations replicating the same experimental tests. The ES and AS dustiness testers require differing operating conditions to follow their respective standards. This condition will be presented in this study without air flow in the rotating drums of both dustiness testers.

The ES dustiness tester [7] consists of a 300 mm internal diameter stainless steel drum which is tapered at either end to aid in containment of the test material, as shown in Fig. 1(a). There are 8 longitudinal vanes evenly spaced around the circumference within the drum to promote the lifting of the test sample. Each test requires 35 cm^3 of material to be placed in the drum, after which the drum rotates at 4 rpm for a period of 1 minute.

The AS dustiness tester [8] consists of a 300 mm internal diameter and is tapered at the back of the drum. This drum is made from stainless steel which has a vertical front wall constructed of a Perspex plate, as shown in Fig. 1(b). There are 8 longitudinal vanes evenly spaced around the circumference within the drum to promote the lifting of the test sample. Each test requires 1000 cm^3 of material to be placed in the drum, after which the drum rotates at 29 rpm for a period of 10 minutes.

The experiments of both dustiness testers were operated at their specified rotational speeds and volume of test sample and the location of the initial sample was placed evenly from the front to the back of each drum.

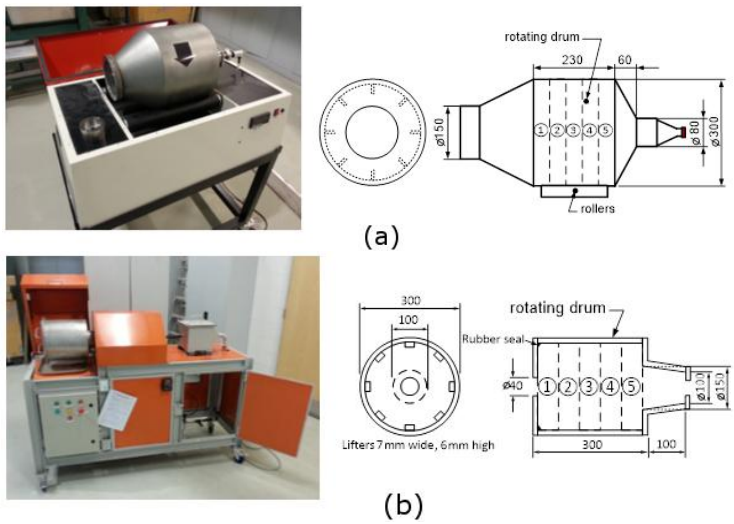

Fig. 1. (a) European Standard dustiness tester [7] and (b) Australian Standard dustiness tester [8].

3. COMPUTATION MODELS

In recent years, numerical simulation has become one of the most useful techniques for modelling particle flows. The DEM method has been developed and widely used to study interactions between the particles and their environment.

3.1 Modelling of solid motion

Particles flowing in rotating drums have been described in many references [15-17]. The motion of each particle is based on rotational and translating motions according to Newton's second law. The equations are as follows.

$$m_i \frac{dv_i}{dt} = \sum(F_{ij}^n + F_{ij}^s + m_i g) \tag{1}$$

$$I_i \frac{d\omega_i}{dt} = \sum_j (R_i \times F_{ij}^s - \mu_r R_i \left|F_{ij}^n\right| \widehat{\omega_i}) \tag{2}$$

where m_i, I_i, v_i and ω_i are the mass, the moment of inertia, translational velocities and rotational velocities of particle i, respectively. F_{ij}^n, F_{ij}^s and $m_i g$ represent the normal contact force, the tangential contact force imposed on particle i by particle j and gravitational force, respectively. R_i represents a vector from the centre of particle to contact surface, μ_r represents the coefficient of rolling friction and $\widehat{\omega_i}$ is a unit vector equal to ω_i divided by its magnitude. The contact force model between the particles and particle-wall are based on a spring-dashpot model and Hertz-Mindlin no-slip model. The magnitude of the normal force between two particles is given as [16]:

$$F^n = -k_n \Delta x + C_n v_n \tag{3}$$

The magnitude of the tangential force is given as:

$$F^t = \min[\mu F^n, k_t \int v_t dt + C_t v_t] \tag{4}$$

where k_n and k_t are the normal stiffness and tangential stiffness respectively, Δx is the particle overlap, v_n and v_t are relative normal velocity and relative tangential velocity respectively, C_n and C_t are the normal damping coefficient and tangential damping coefficient respectively, C_n depends on the coefficient of restitution, e defined as the ratio of the normal component of the relative velocity after and before the collision.

$$C_n = -2\ln(e) \frac{\sqrt{m_{ij} k_n}}{\sqrt{\pi^2 + \ln^2(e)}} \tag{5}$$

$$m_{ij} = \frac{m_i m_j}{m_i + m_j} \quad (6)$$

where m_{ij} is the reduced mass of two particles i and j. In addition, the DEM simulations investigate the particle contact stress, particle collision and energy dissipation occurring when material flows and impacts in the ES and AS dustiness testers. The interaction of particle contact effect from the coefficient of static/rolling friction between particle-particle and between particle-wall will be considered. The interaction force between particle-particle and particle-wall are analysed to understand their influence in terms of typical flow features in rotating drums, particle collision frequency and collision energy under different particle size are considered in the axial and radial directions.

3.2 Methodology analysis

Iron ore and coal were chosen as the test material for this investigation to visualise the contact stress and energy dissipation when material impact on the other particles or the wall of the drums of the two dustiness testers, but do not to measure the amount of dust generated during the testing. This is also vital for the DEM simulations replicating the same experimental tests. The ES and AS dustiness testers require differing operating conditions to follow their respective standards, see Section 2.

4. SIMULATION CONDITION

The geometry of the dustiness testers and type of particles used in these simulations were based on the experimental work. To produce accurate DEM simulations, the physical properties of the materials and the drums (304 stainless steel) have been used to aid in the determination of the interaction properties, as shown in Table. 2. The processes used for many of these tests has been reported previously [18, 19], including the particle shape and particle size of the particle model used in the DEM simulations. Subsequently, in the DEM simulations the particles were set with a fixed spherical particle size.

The particle shape and particle size of the iron ore and coal particles were more irregular and dimensions hard to determine by measurement of the materials. Particle models were based on equivalent volume diameter and mass of the particles. The simulated volume and mass of the particle model was matched with the experimental data. Subsequently, particle models in the DEM simulations were set with a fixed size and shape. All particles were generated from an injection plane and allowed to fall due to gravity alone to the bottom of the drum in 2 sec. The particle size and particle shape of the coal model, material properties and interaction between particle-particle and between particle-wall selected for simulation by DEM software for the two dustiness testers are shown in Table. 2.

Table 3 summarises the dimensions and number of particles required for the four particle sizes used in the rotating drum simulations. The $P_{6.3}$ particle is representative of the larger sized particle measured experimentally at an equivalent volume diameter of 6.3 mm while $P_{5.6}$, $P_{4.0}$ and $P_{2.0}$ are arbitrarily smaller sized particles of equivalent volume diameters of 5.6 mm, 4.0 mm and 2.0 mm, respectively.

The calculation of the required number of particles was based on experimental data (Table 3) of the particle samples tested in both dustiness testers. A simplification was made in the calculation of the number of particles required, that being there was no accounting for the void space that would exist between the particles. The simulation configurations are built to match the experiment with equal the mass and volume of material 35 cm^3 for the ES dustiness tester and 1000 cm^3 for the AS dustiness tester.

Table 2: Properties of iron ore, coal, stainless steel and Perspex

Properties	Iron ore	Coal	Stainless Steel	Perspex
V (m^3)	0.101	0.107	-	-
M (g)	0.276	0.132	-	-
ρ_s (kg/m^3)	3867.8	1422.4	8000	1200
ν	0.4	0.35	0.29	0.35
G (GPa)	1.92E8	9E8	7.75E10	1E9
CoR	0.258	0.55	0.6	0.58
μ_s	0.58	0.6	0.4	0.43
μ_r	0.1	0.1	0.3	0.3

Note: V is the particle volume; M is the particle mass; ρ_s is the particle density; ν is the Poisson's ratio; G is the shear modulus; CoR is the particle coefficient of restitution; μ_s is the particle coefficient of static friction and μ_r is the particle coefficient of rolling friction.

Table 3: Dimensions of simulated particles and the number of particles required for the DEM simulations

	Number of Particles			
	Iron Ore		Coal	
d (mm)	**ES**	**AS**	**ES**	**AS**
$P_{6.3}$	6	164	18	510
$P_{5.6}$	39	1155	51	1450
$P_{4.0}$	355	10385	262	7470
$P_{2.0}$	1025	29825	450	12800

5. Results and Discussion

In this study the behavior of particles flow in an EN 15051 and AS 4156.6 rotating drum has been investigated via experimental tests and DEM simulations. The validity of the DEM model used was confirmed by comparing simulation and experimental results in terms of the flow patterns observed was shown in a previous paper [19].

5.1 Particle impact stress

When a particle falls and impacts on the drum wall or other particles at an impact velocity (v_p), that particle has an impact stress (σ_1). If the impact stress (σ_1) is larger than the particle strength (σ_s), the result is particle breakage and particle strength (σ_s) is determined by Griffith's theory [9]. Particle contact stress (σ_1) for the spherical particle impacts on the drum wall or on other particles is determined by talking the maximum load impact in the drum and dividing by the projected area of a particle. This results in the average contact stress of the particle impact in the rotating drum per second, as shown in Fig. 2. For the ES dustiness tester, the results are shown in Fig. 2(a). It can be seen that the particles with higher particle density produce the higher contact stress. The particle movement in the drum is as a result of two different motions, particles moving on the drum wall and falling from the vanes to the bottom of the drum. The particles start moving up on the drum wall via the vanes in the drum, but in this section, forces are not generated on each particle and the velocity of the particles is the same as the drum as it rotates. The particles falling from the vanes display the highest force acting on the bottom wall and create the high contact stress on each particle. The particle movement in the AS dustiness tester is shown in Fig. 2(b). It can be seen that the contact stress of the iron ore and coal have very similar trends over the simulation time. Both materials vary particle size in the range 2.0 mm to 6.3 mm, but the density of the iron ore is higher than coal so the iron ore shows a higher contact stress.

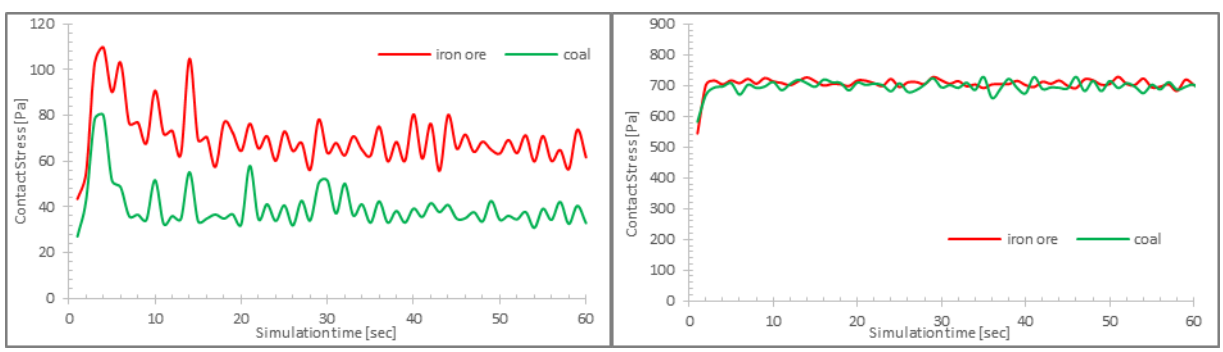

(a) (b)

Fig. 2. Contact stress on the particles in the (a) ES dustiness tester (b) AS dustiness tester.

5.2 Force structure in the dustiness testers

Particle flow mechanisms which have been identified in the dustiness tester are directly related to the contact forces on other particles and drum wall, as related to [20]. It is important to quantify the forces between particle-particle and between particle-wall interactions. In this section, the magnitude of three forces was analysed: the average normal contact force and average tangential contact forces, the maximum normal and tangential contact forces and

the total normal and tangential contact forces of all particles per time step over the simulation time in the dustiness testers. The average particle force at a contact with another particle or the drum wall is calculated by the contact particle force at a given time step according to equations (3) and (4). The maximum force in a contact of a particle in the dustiness tester can be determined according to the value of the maximum particle force in the drum for each time step. The total particle forces in the dustiness tester are the sum of all contact forces between particles and between particles and drum wall per time-step. Fig 3 shows the particle distribution in the ES dustiness tester of the contact force with different particle sizes. In Fig 3(a) it is evident that large normal contact forces are occurring on the particles falling from the vanes and impacting on the drum wall or other particles. The high peak of the force took place when the particles of higher density fall and impact on the drum wall. Relatively large forces can also be found on the bottom wall of the drum, where particles with high velocities impact on the drum wall and move with different velocities. The tangential force occurring in the ES dustiness tester is shown in Fig 3(b). When the particles contact other particles or the drum wall, the tangential force is the force from the particle displacement of the contact point to the point at the contact end or the point at which the particles begin to roll or slip. Particularly, the highest velocity in the drum has been shown to be the highest force as compared with a different particle size, as shown in Fig 3(c). It can be seen that increasing the size of the particle increases the contact force when the particles fall and impact on the drum wall. However, the contact force occurring between particle-particle depends on their relative velocity. That means the particles at high velocities may not create the highest contact force if their relative velocity is small. Therefore, the contact force is not necessarily correlated with the velocity of the particles; it should be based on the systems and operating. However, the size of particle and percentage of particle volume fraction or mass of particle fraction were an influence on the contact force during the drum rotation.

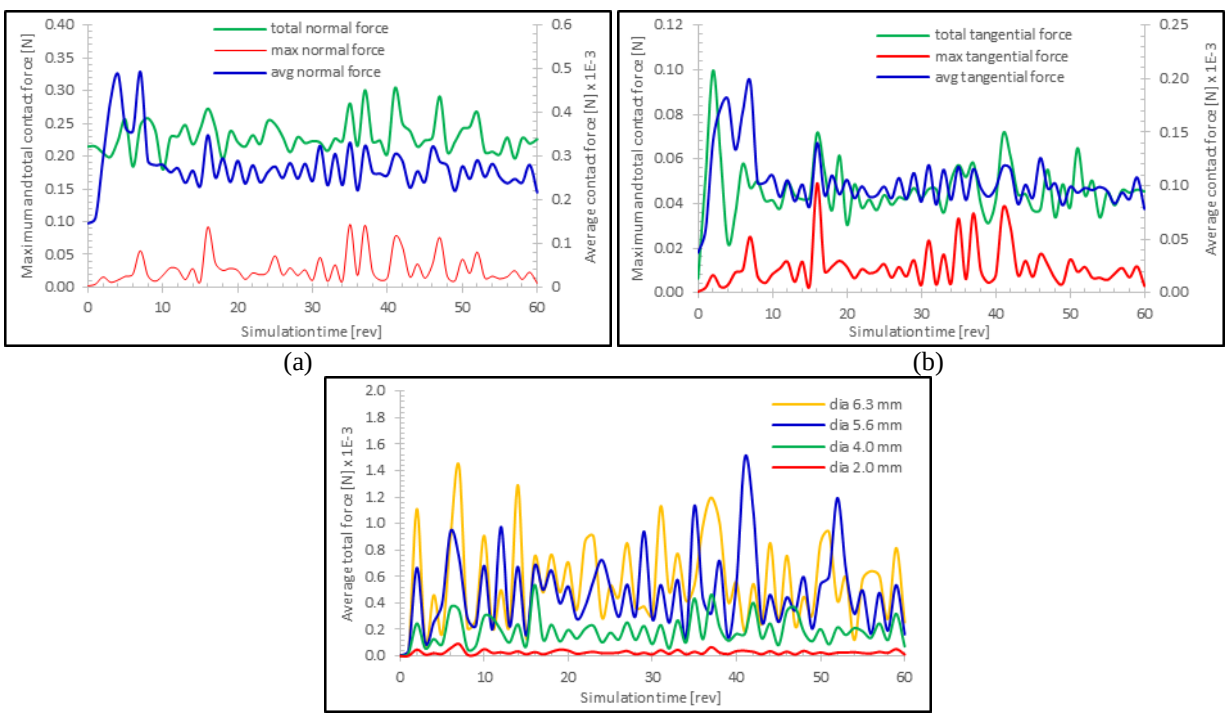

Fig. 3. The distributions of the particle contact in the ES dustiness tester (a) normal contact force (b) tangential contact force (c) total normal contact force.

Fig 4 shows the particle contact force distribution in the AS dustiness tester. Fig 4(a) gives the average contact normal force occurring on the particles which are in direct contact with one another or with the drum wall. It can be seen that most of the forces generated in the dustiness tester are steady-state for the entire simulation time. However, the particle displacement of the contact from the first point to the end of the contact point before that particle begins rolling or slipping is called the tangential contact force, as shown in Fig 4(b). Fig 4(c) shows the average total contact force of particle acting in the dustiness tester as compared with different size of particles moving within the rotating drum over the entire simulation time.

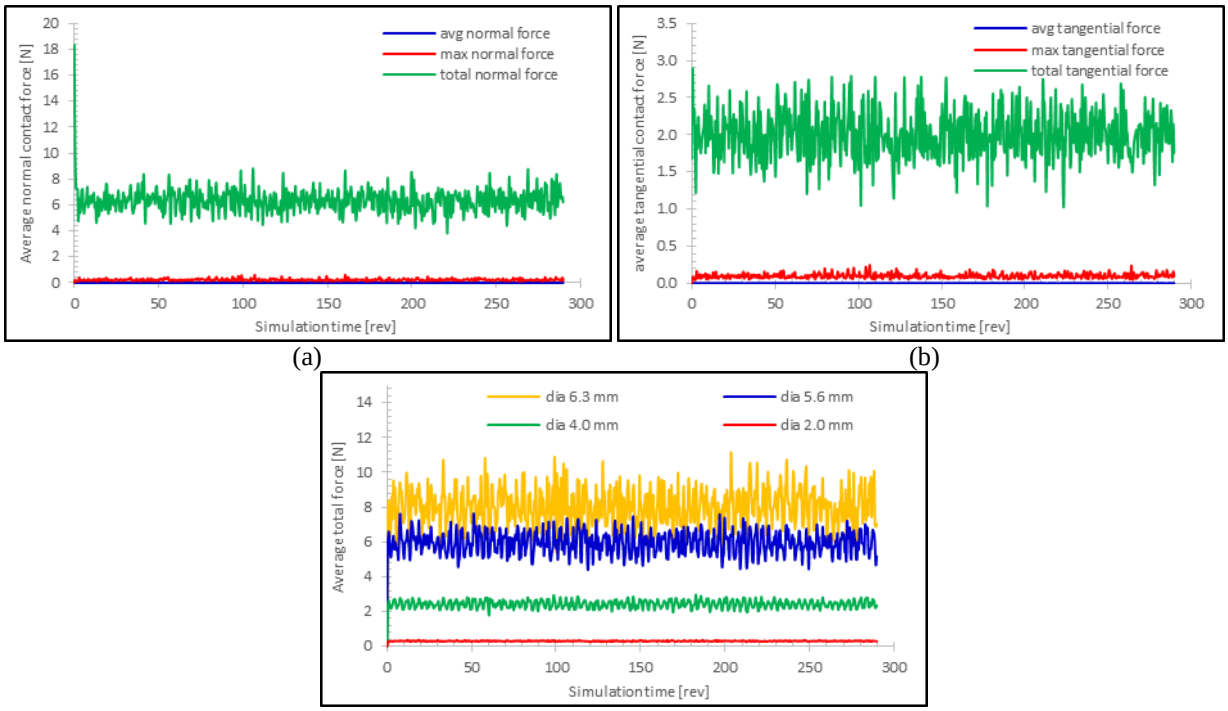

Fig. 4. The distributions of the particle contact in the AS dustiness tester (a) normal contact force (b) tangential contact force (c) total normal contact force.

5.3 Collision energy and frequency

The energy loss in the dustiness tester depends on the particle-particle and particle-wall interactions. The normal energy loss is defined as the energy loss during a particle collision with another due to normal direction overlap. The tangential energy loss is defined as the energy lost during a particle collision with another particle or the drum wall due to the tangential overlap. Total energy loss is the sum of the normal and tangential energy loss due to the particle collisions. These factors are impossible to quantify in a physical experiment. In this section, a numerical method by DEM simulation was used. Using this method, the motion of particles and their interactions with others, and the energy dissipation when the particle collision can be determined. The energy losses in the normal and tangential direction, collision energy and collision frequency were determined from all particle collisions in the drum. Fig. 5 shows the number of particle collisions and average energy loss in the ES dustiness tester. Fig. 5(a) shows the number of particle-particle and particle-wall collisions in the drum. The initial transient behaviour of the particles shows peak values as all particles fall together to the bottom of the drum before steady-state conditions establish after 1 revolution of the drum. It is clearly seen that the particle-particle collisions have a higher value than the particle-wall collisions due to the formation of the bed of material involving many particle interactions. Fig. 5(b) shows the average energy loss per time-step of all particles moving in the ES dustiness tester. The particles falling from the vanes and impacting on the lower surface of the drum is higher than the particle movement on the wall surface of the drum as it rotates. In regards to the behaviour of particle flow in the AS dustiness tester, most particles slide on the wall of the drum as it rotates. Fig. 6(a) displays the number of particle-particle and particle-wall collisions and it can be seen that there are many more particle-particle collisions. For the average energy loss per time step, as shown in Fig. 6(b), it can be seen that the energy loss is steady-state over the simulation time (after the initial transient period) and the normal and tangential energy loss are very similar as to the energy loss as the drum rotates.

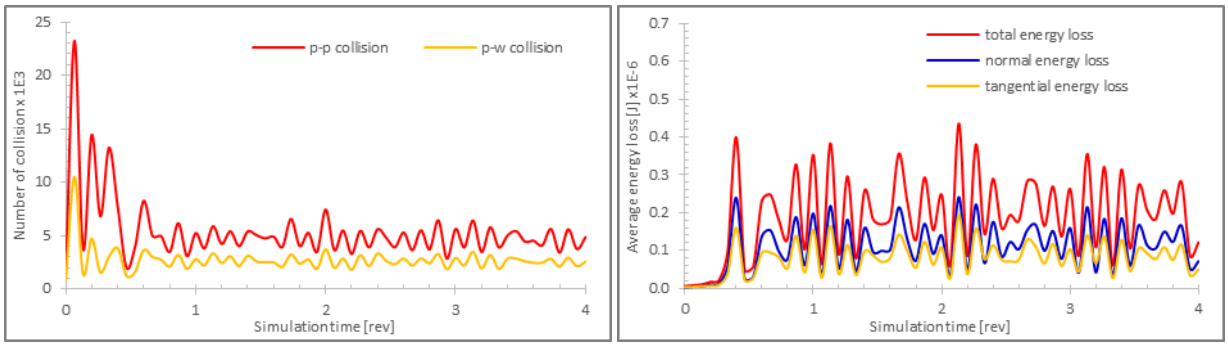

(a) (b)

Fig. 5. The distributions of particle collision in the ES dustiness tester (a) number of collision (b) energy loss of particle.

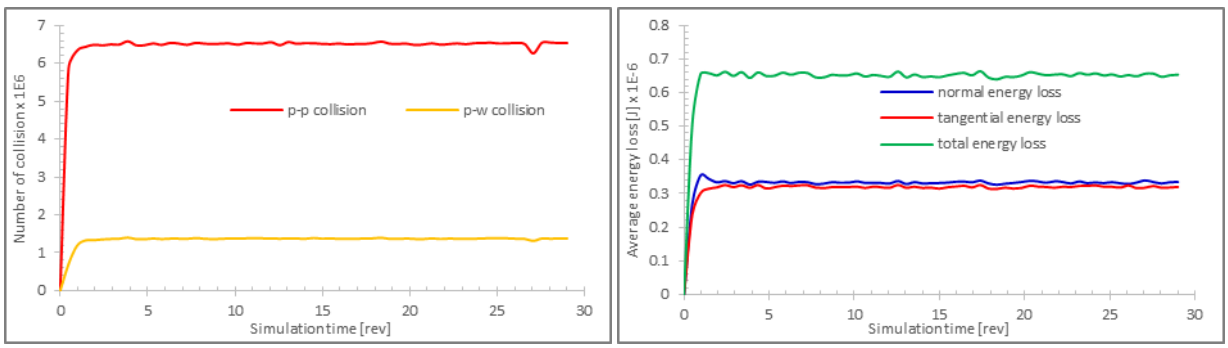

(a) (b)

Fig. 6. The distributions of particle collision in the AS dustiness tester (a) number of collision and (b) energy loss of particle.

Additionally, the particle flow in the ES and AS dustiness testers will be analysed in terms of collision energy (C_E) and collision frequency (C_F). The collision energy is defined as the collision energy per collision of a particle within a second. Both particle-particle and particle-wall collision energy in terms of kinetic energy are calculated by $C_E = \frac{1}{2} m_i v_{ij}^2$, where m_i is the mass of particle and v_{ij} is the relative velocity of two particles ($v_{ij} = |v_i - v_j|$) when the particle comes into collision with another particle or between particle and the wall of the drum; it is the relative collision velocity between the two objects. For the collision frequency in the dustiness tester is defined as the number of collisions per particle as recorded per second. Fig. 7 displays the energy of particle distribution in the ES dustiness tester. Fig. 7(a) shows the average of the collision energy and collision frequency of the particle flow in the ES dustiness tester. The peak location of the particles distributing the collision energy corresponds to the location of the high density of particle collisions. At the bottom wall of the drum, particles moving with the drum rotation have the same velocity as that of the drum. Particles on the vanes, before falling to the bottom drum, are relatively densely-packed and there are a rapid series of collisions with their neighbours, leading to high collision frequency. On the other hand, after particles move out from the vanes to the bottom drum wall, there is a relatively long distance before they collide with other particles or the drum wall, leading to a low collision frequency. Fig. 7(b) and Fig. 7(c) show the collision energy and collision frequency occurring in the different particle sizes over the simulation times. The large particle size movement in the rotating drum produces the highest energy loss compared to the other particle sizes. Fig 7(d) shows the average particle-particle and particle-wall collisions velocity as a function of the simulation time. It clearly is seen that the collision velocity between particle-particle and between particle-wall were very similar in their trends over the simulation time. The peak of collision velocity is recorded in the particle falling and impact on the bottom drum wall. The low collision velocity of the particles corresponds to the particles moving up via the vanes from the bottom to the top angle of the drum rotation before the particles again fall to the bottom of the drum. In the ES dustiness tester, the peak average particle–particle collision velocity is 0.102 m/s, which is 14% higher than in the average relative velocity of particle-wall collisions.

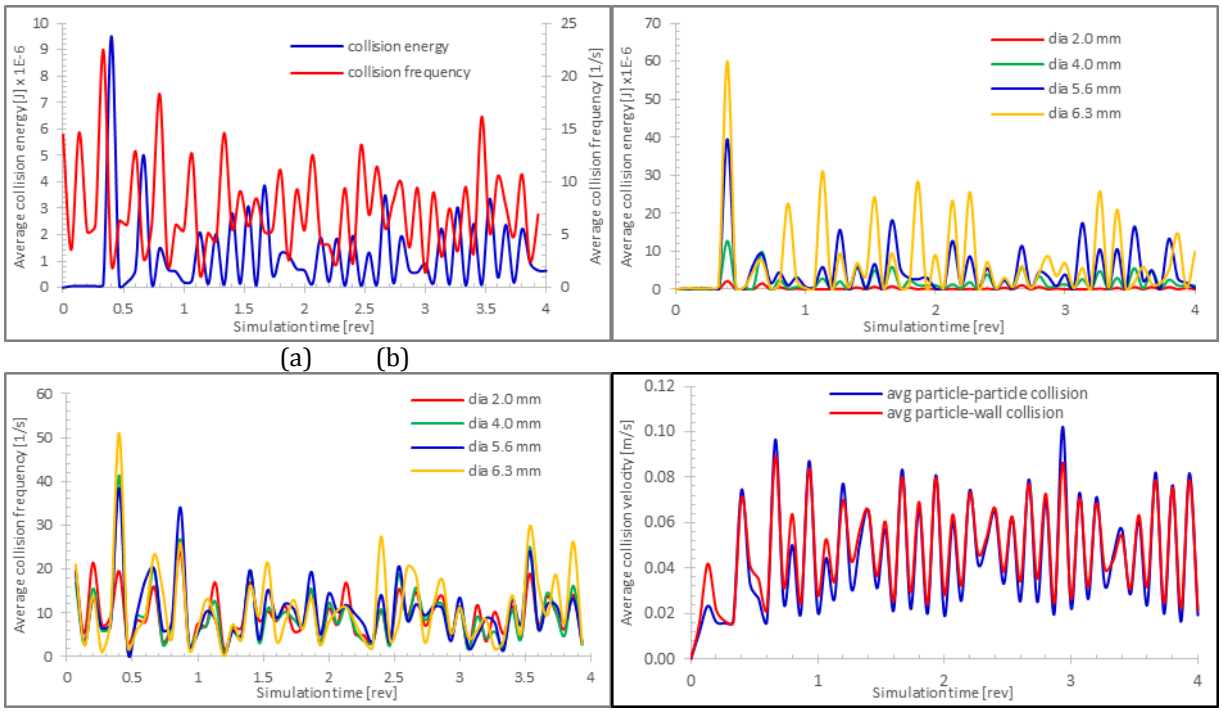

Fig. 7. Energy of particle distribution in the ES dustiness tester (a) collision energy and collision frequency for the all particle size (b) collision energy and (c) collision frequency for the different particle size.

Fig. 8 displays the energy of particle distribution in the AS dustiness tester. Fig. 8(a) shows the average collision energy and collision frequency of all particle sizes flowing in the drum. The distribution of all particles is steady-state after the drum rotates 2 revs. Fig. 8(b) and Fig. 8(c) show the collision energy and collision frequency for the four particles of different sizes in the range of the simulation time into the steady-state condition. Fig 8(d) show the particle-wall collision velocity has a cyclic trend over the whole simulation time, the average particle-wall collision velocity is 46% higher than in the average velocity of particle-particle collisions.

It can be clearly seen that the collision energy and collision frequency increases as the particle size increases, based on the number of particles moving in the system. Fig. 9 shows the average collision energy and collision frequency with different particle sizes moving in the drum with five locations (bins) in the ES dustiness tester. It can be seen that high collision frequency does not necessarily always correspond to high collision energy. The average collision energy and collision frequency were calculated for each particle size and five location bins. This calculation is carried out for the simulation time t = 60 sec. The results are, finally, average values of the collision energy and collision frequency over simulation time. Fig. 9(a) shows that the particle distributions in the ES dustiness tester combining high collision energy with low collision frequency (Fig. 9(b)) corresponds to each section of five bins and peak of collision energy at the middle drum (bin3) where particles obtain high velocities due to falling from the lifting vanes. The low collision energy corresponds to both sections close to the end wall (bin1 and bin5) and highest collision frequency at the bin1. This is the particle collision all the time before particles begin sliding on the cone wall of the drum.

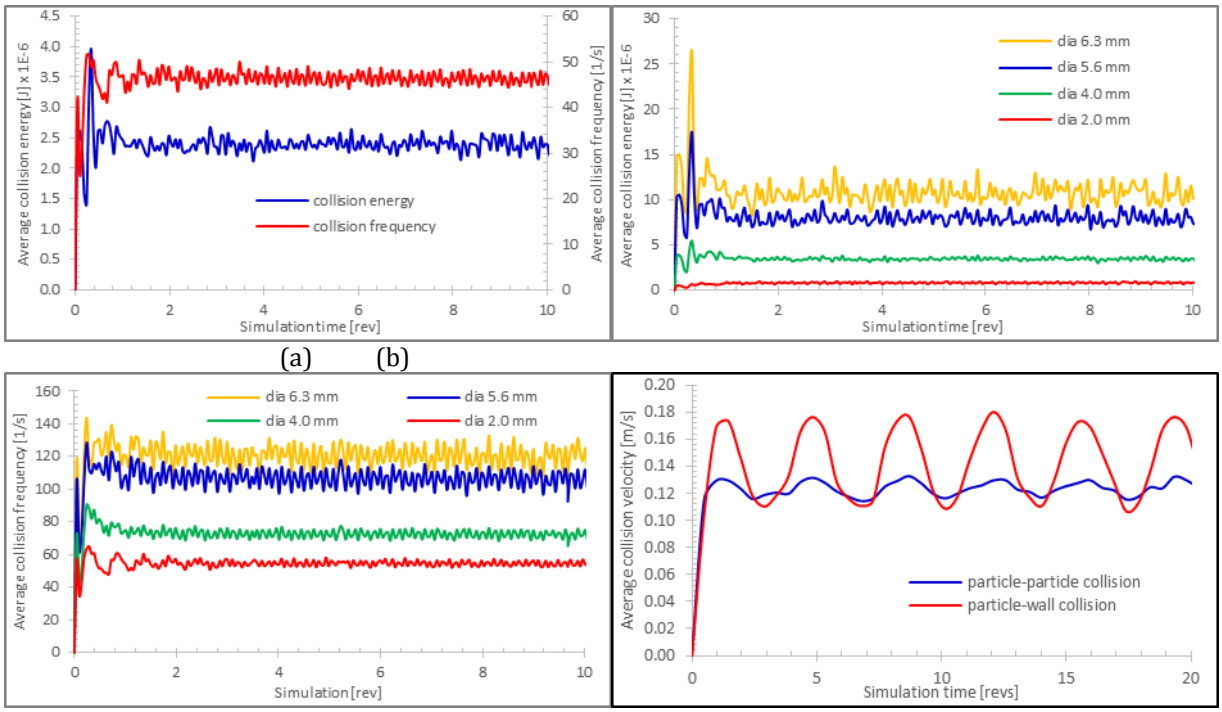

Fig. 8. Energy of particle distribution in the AS dustiness tester (a) collision energy and collision frequency for all particle size (b) collision energy and (c) collision frequency for the different particle size.

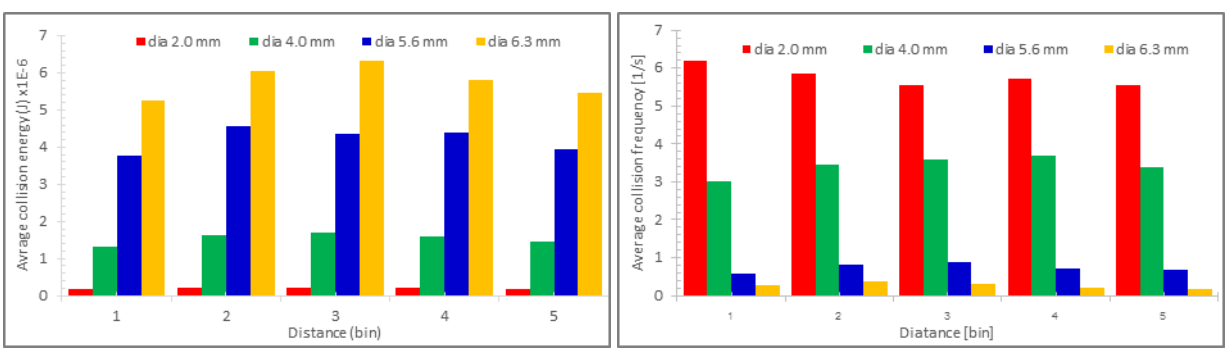

Fig. 9. The particle distributions in the ES dustiness tester with different particle sizes and 5 bin positions (a) average collision energy (b) average collision frequency.

Fig. 10 shows the average collision energy and collision frequency with four particle sizes and 5 bin positions in the AS dustiness tester. The results are an average collision energy and collision frequency record when the particle flow is steady-state at the simulation time t = 60 sec. Fig. 10(a) displays the highest collision energy occurring on the large particle size at both end walls of the rotating drum. The collision energy and collision frequency are both affected by the vertical end wall blocking the other particles moving in the axial direction of the rotating drum. The highest collision frequency occurs on the small particle size at both end walls of the drum. Like for the ES dustiness tester, both collision energy and frequency are related to many factors, including static friction and rolling friction of the particles, movement of the particles and operating conditions of the dustiness tester. Fig. 10(b) suggests the high collision frequency does not necessarily always correspond to high collision energy.

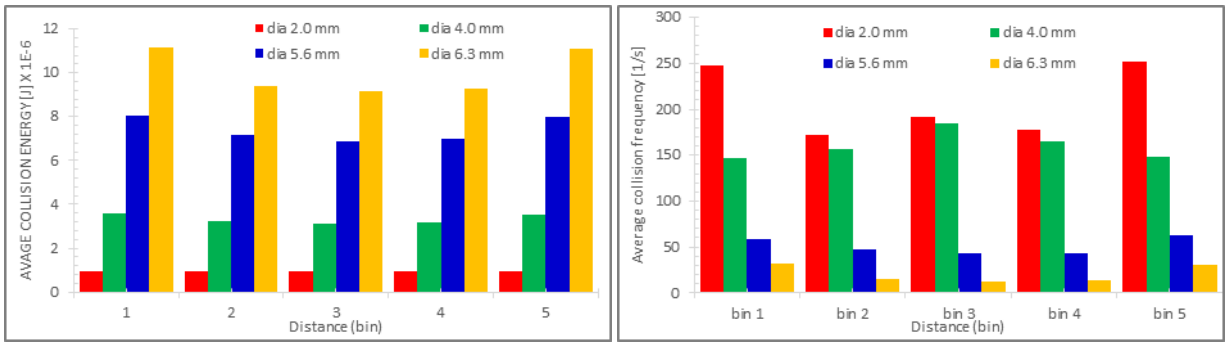

(a) (b)

Fig. 10. The particle distributions in the AS dustiness tester with different particle and 5 positions (a) average collision energy (b) average collision frequency.

5.4 Particle size distribution

In this section four distinct particle sizes have been used to observe the effect of size distribution in the dustiness tester simulations. The size of the particles effects the particle flow patterns significantly when the coefficient of static/rolling friction between particle and particle interaction and between particle and wall interaction. The small particles are collected and move to the middle of the drum faster when $\mu_{s(p,p)}$ drops to the lower values. The particles change the $\mu_{r(p,p)}$ to the lowest values, the small particles are collected and move together in the rotating drum. As $\mu_{r(p,p)}$ increases, less small particles are lifted in the moving heap. The particles free fall from the vanes at higher angles and small sized particles very quickly move to the middle of the drum when $\mu_{s(p,w)}$is increased. The flow patterns of particle flow are very similar with all different sized particles moving in the rotating drum when $\mu_{r(p,w)}$ is changed.

Due to granular particle segregation, the smaller particles move downward through the rotating heap of particles through the voids between particles. The particles are lifted on the vanes, the large particles fall first and the last particles to fall from the vanes are mostly the smallest particles. These small particles fall close to the vertical centerline of the drum. Fig. 11 shows the particle size distribution of iron ore segregation in the middle section (bin3) in the ES dustiness tester at different times and the number of particles, as shown in Table 3. Fig. 11(a) shows the influence of different particle size in the ES dustiness tester. It can be seen that for large particle sizes greater than 5.6 mm, there is variance for the entire simulation. The reason the graph of 6.3 mm diameter particles looking different to the others in Fig. 11(a) is due to the relatively small number of particles in this size range. For particle sizes lower than 4.0 mm, there was very constant moving in the middle section of the rotating drum for the entire simulation. Fig. 11(b) shows the particle sizes distribution in the five bins of the ES dustiness tester at the end time t = 60 sec. The particles are moving from both end walls towards the centre of the rotating drum.

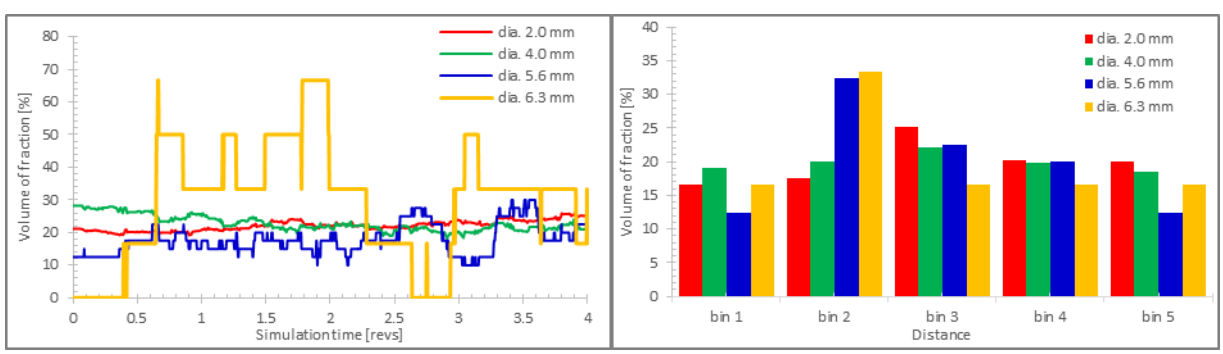

(a) (b)

Fig. 11. Particle size distribution in the ES dustiness tester at (a) the middle of the drum (bin3) and (b) the axial size distribution of particles in the drum at time t = 60 sec.

For the AS dustiness tester is show in Fig. 12. Fig. 12(a) shows the small particle size movement in the middle section (bin3) of the rotating drum. In Fig. 12(a), it can be seen that there is a very transient behaviour of all particle sizes in the first 20 revs of the simulation. After this time, the different size fractions begin to move axially through the bin. The large particles (5.6 and 6.3 mm diameter) have nearly all left bin3 by the completion of 80 revs. The 4 mm particles have reduced in number by 80 revs and the number of 2 mm particles has increased dramatically by 80 revs. After 80 revs until the end of the simulation, the number of each particle size reaches a steady state condition. Fig. 12.(b) shows the large particle size movement to the end walls of the drum (bin1 and bin5) and small particle size present in the middle (bin3) of the rotating drum. As can be seen, each different particle size has a different trend along the length of the drum. The number of 2 mm particles increases towards the centre of the bin. The number of 4 mm particles initially rises from bin1 to bin2 and bin5 to bin4 the drops again in bin3. The number of 5.6 mm and 6.3 mm particles drops dramatically from the centre (bin3) of the drum towards the front and back of the drum.

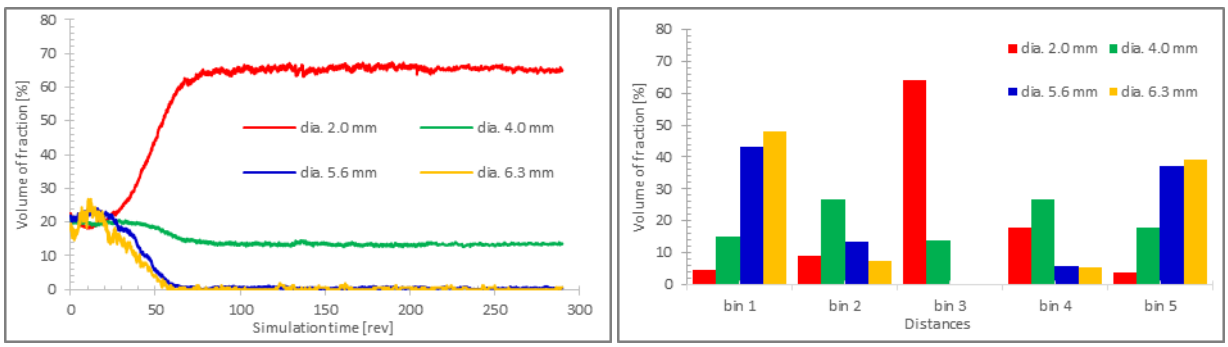

(a) (b)

Fig. 12. Particle size distribution in the AS dustiness tester at (a) the middle of the drum (bin3) and (b) the axial size distribution of the particles in the drum after 80 revs.

5.5 Energy dissipation

The impact energy referred to as the kinetic energy, is calculated by

$$E_{imp} = \sum_{i=1}^{n} \frac{1}{2} m|V_r|^2 \quad (7)$$

where m is the particle mass, V_r is the relative velocity for a particle and particle or a particle and wall collision and n is the total number of collisions. The impact energy generated within the exact time has a distribution, depending on the particle size and operating conditions of the drum as it rotates. This impact energy is calculated by the kinetic energy of all particle contacting is summed up for all the contact points within 1 sec but the kinetic energy during contacting is not calculated. Accordingly, the impact energy thus obtained corresponds to the maximum kinetic energy of particles at the collision per unit time.

The impact energies dissipated during collisions between particles, between particles and vanes/wall can be measured and recorded at any angular position as a function of time during a drum revolution. The normal component of the relative velocity represents a particle falling from the vanes to the lower drum. Apart from that, the tangential force is related to normal force through the friction coefficient. Therefore, impact energy in the shear direction has already been included in the calculations. Fig. 13 shows the distribution of particle impact energies in the ES dustiness tester on other particles or the drum wall for the two material models. It can be seen that the DEM simulations can predict impact energy occurring on the individual particle movement in the rotating drums.

Impact energy is defined as collision energy per collision of a particle on other particles or the drum wall within 1 second. Fig. 14 presents the average impact energy per unit time for the ES dustiness tester. After the drum has undergone 0.5 rotations, there is a noticeable energy increase with more density packing and particles falling from the vanes to the lower part of the drum. The impact energy of both materials all show similar trends of energy increase when the particles drop to the drum wall and do not generate energy as the particles are lifted by the vanes. This process is repeated until the simulation end time. The energy dissipation of each particle model increases with

the increase of particle velocity. The range of energy dissipation depends on the range of particle size flow in the drum. The iron ore and coal have a wider range of particle sizes, as the particle velocity increased with the 4 different particle sizes moving in the rotating drum. For the ES dustiness tester, there is a small amount of particle flow in the drum (small test sample size), so approximately 50% of the particles are falling from the vanes to the drum wall every 2 sec. The highest impact energy occurs with the particle impact on the drum wall. The experimental impact energy was unable to be measured and hence no comparison can be made for the simulated energy dissipation.

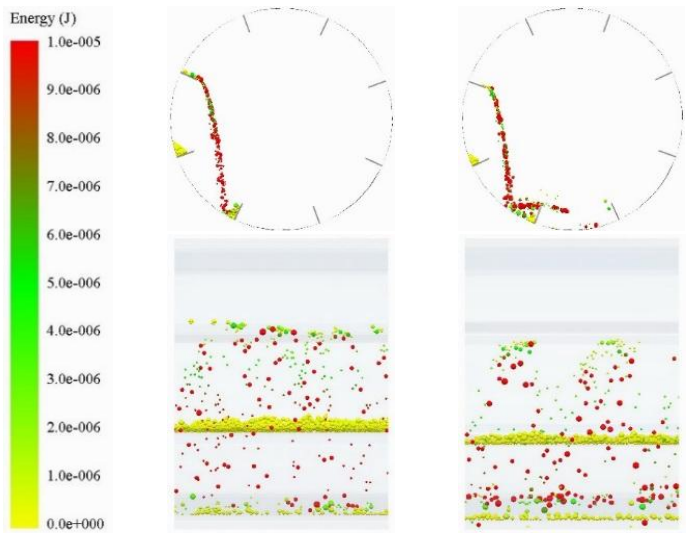

(a) (b)

Fig. 13. The distribution of particle impact energies in the ES dustiness tester at 30 sec for (a) iron ore and (b) coal.

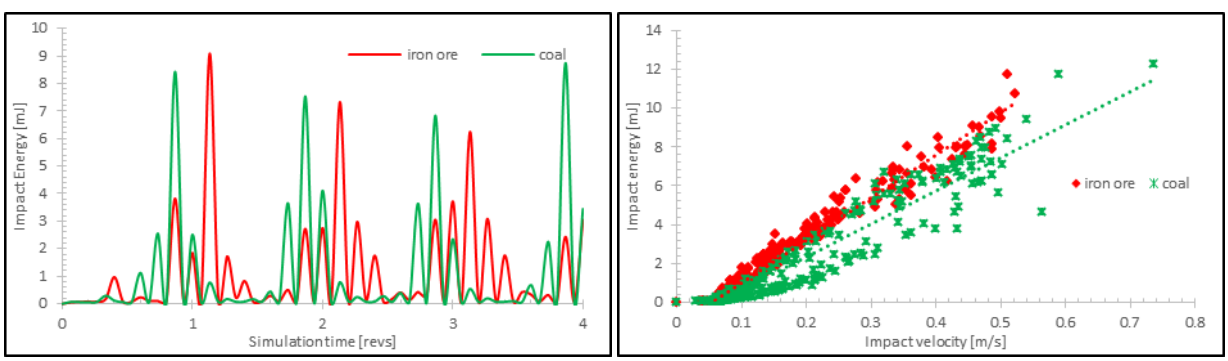

(a) (b)

Fig. 14. Shows the impact energy in the ES tester (a) over the simulation time and (b) per impact velocity.

The particle impact energy in the AS dustiness tester is shown in Fig. 15. There are two material models shown in the AS dustiness tester at steady-state conditions (at t = 10 sec). It can be seen that as the solid density increases, the energy and more amount of particles are greater than 0.1 mJ of the energy dissipation in the drum. There is more energy generated on the particle impact on the free surface of the particles moving in the drum as it rotates. The iron ore and coal show very similar trends of particle flow in the rotating drum. The small sized particles move up to high angular positions before dropping to the free surface. The iron ore has the higher density and results in the falling particles having a higher impact force on the particles in the moving bed, as can be seen in Fig. 15.

Fig. 16 shows the average impact energy per second for the particle impacts and rebounds and the velocity of the particles with respect to their energy during the contacts of each particle. Fig. 16(a) displays the distribution of the impact energy for the both material models and can be seen to be very steady-state over the simulation time. The iron ore and coal have the same particle size range (2.0 – 6.3 mm), but different solid densities and different

amounts of particles for each size range of material. The iron ore has the higher particle density and also recorded the higher impact energy when compared to coal. In addition, Fig. 16(b) shows the particle velocity increases the effect of the impact energy in the rotating drum. The materials falling and sliding on the free surface show the velocity of iron ore particles in the range of 0.294 - 0.355 m/s is lower than for coal and records impact energy in the range of 2.82 – 3.47 mJ is greater than coal. For the coal, the impact energy increases from 1.93 to 2.85 mJ as the velocity increases from 0.355 to 0.429 m/s.

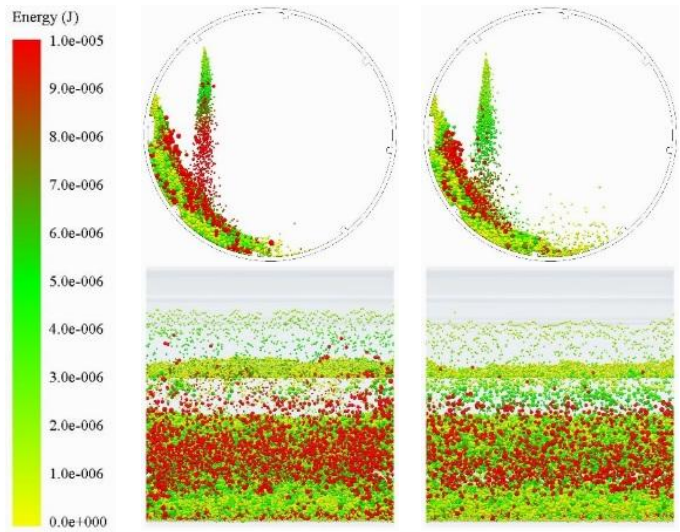

(a) (b)

Fig. 15. The distribution of particle impact energies in the AS dustiness tester at 10 sec for (a) iron ore and (b) coal.

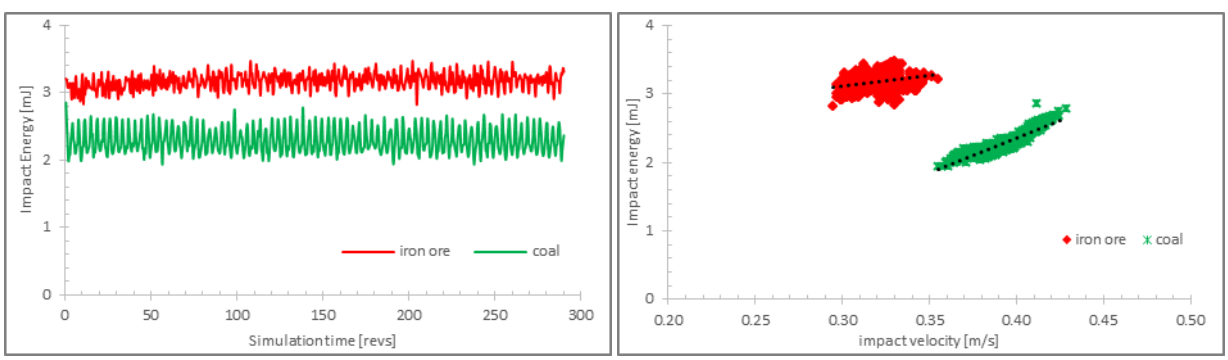

(a) (b)

Fig. 16. Shows the impact energy in the ES dustiness tester (a) over the simulation time and (b) per impact velocity.

6. CONCLUSIONS AND FURTHER WORK

In this study, the energy dissipation of particles during impact in an EN 15051 and AS 4156.6 rotating drum have been investigated via DEM simulations. While the particles start moving up on the drum wall via the vanes in the drum, forces are not generated on each particle. The velocity of the particles is the same as the drum as it rotates. The particles falling from the vanes display the highest force acting on the bottom wall or other particles and create high contact stresses on each particle. The impact stress on the drum wall or on other particles of the iron ore and coal have very similar trends over the simulation time.

The energy loss in the dustiness tester depends on the particle-particle and particle-wall collisions. The peak location of the particles distributing the collision energy corresponds to the location of the high density of particle

collisions. The collision energy and collision frequency both increase as the particle size increases, based on the number of particles moving in the system. The impact energy of both materials shows similar trends of energy increase when the particles drop to the lower drum wall and do not generate energy as the particles are lifted by the vanes. The energy dissipation of each particle model increases with the increase of particle velocity. For the ES drum, the highest impact energy occurs with the particle impact on the drum wall. For the AS drum, there is more energy generated by the particle impact on the free surface of the particles moving in the drum as it rotates. The iron ore has the higher particle density and also recorded the higher impact energy when compared to coal.

The size of the particles effects the particle flows patterns significantly when the coefficient of static/rolling friction changed. The small particles are collected and move to the middle drum faster when $\mu_{s(p,p)}$ drops to the lower values, and move with the vanes and rotate to higher angles when $\mu_{s(p,w)}$ increased. When the $\mu_{r(p,p)}$ changes to the lowest values, the small particles are collected and move together, and the flow patterns of particle are very similar with all different sized particles moving in the rotating drum when $\mu_{r(p,w)}$ is changed.

7. ACKNOWLEDGEMENT

The authors would like to thank the Thailand Government and University of Wollongong, Australia for their financial support, which has allowed this research to be pursued.

REFERENCES

[1] Wypych, P.W. and Cooper, P. Improving Dust-Fume Control, in 5th International Conference on Bulk Materials Storage, Handling and Transportation, Australia, 1995.
[2] Chen, X.L. et al. Modelling Dust Emissions from Belt Conveyor Transfer Chutes, Bulk Solids Handling, 29 July 2014.
[3] Frew, I., Wypych, P.W. and Mar, L. Different Modes of Dust Testing for Bulk Solids, in 11th International Conference on Bulk Materials Storage Handling and Transportation, University of Newcastle, Australia, 2-4 July 2013.
[4] Wypych, P.W., Cook, D. and Cooper, P. Controlling dust emissions and explosion hazards in powder handling plants, Chemical Engineering & Processing: Process Intensification, Vol. 44(2), 2005, pp. 323-326.
[5] Taveau, J. Secondary dust explosions: How to prevent them or mitigate their effects?, Process Safety Progress, Vol. 31(1), 2012, pp. 36-50.
[6] Hjemsted, K. and Schneider, T. Documentation of a dustiness drum test, The Annals of occupational hygiene, Vol. 40(6), 1996, pp. 627-643.
[7] EN 15051, Workplace Atmospheres. Measurement of the Dustiness of Bulk Materials. Requirements and Reference Test Methods, 2006, Comité Européen de Normalisation. p. 25.
[8] AS 4156.6, Coal Preparation Part 6: Determination of Dust/Moisture Relationship for Coal, 2000, Standards Australia. p. 21.
[9] Smagorinsky, J. General circulation experiments with the primitive equations: I. The basic experiment, Monthly Weather Review, Vol. 91(3), 1963, pp. 99-164.
[10] Leung, K. An energy based, ore specific model for autogenous and semi-autogenous grinding mills, Vol., 1988.
[11] Wang, M.H., Yang, R.Y. and Yu A.B., DEM investigation of energy distribution and particle breakage in tumbling ball mills, Powder Technology, Vol. 223, 2012, pp. 83-91.
[12] Minh, N.H., and Cheng, Y.P. A DEM investigation of the effect of particle-size distribution on one-dimensional compression, Geotechnique, Vol. 63(1), 2013, pp. 44-53.
[13] Wangchai, S., Hastie, D.B. and Wypych, P.W. Particle size segregation of bulk material in dustiness testers via DEM simulation, Particulate Science and Technology, Vol., 2016, pp. 1-9.
[14] Wangchai, S., Hastie, D.B. and Wypych, P.W. Investigation and Modelling of Energy Dissipation of Bulk Materials in Dustiness Tester using DEM, in 7th Thai Society of Mechanical Engineers-International Conference on Mechanical Engineering, Chiang Mai, Thailand, 13 -16 December 2016.
[15] Lili, Z., Zhijun, Z. and Ninghua, K. Granular mixing characteristic 2D simulation in drum dryer by DEM, International Journal of Advancements in Computing Technology, Vol. 4(3), 2012, p. 10.
[16] Paul W. Cleary, Rob Morrisson, and Morrell, S. Comparison of DEM and experiment for a scale model SAG mill, Int. J. Miner. Process, Vol. 68, 2003, pp. 129-165.

[17] Yang, R.Y. et al. Numerical simulation of particle dynamics in different flow regimes in a rotating drum, Powder Technology, Vol. 188(2), 2008, pp. 170-177.
[18] Wangchai, S., Hastie, D.B. and Wypych, P.W. The Simulation of Particle Flow Mechanisms in Dustiness Testers. in 11th International Conference on Bulk Materials Storage, Handling and Transportation. University of Newcastle, Australia, 2-4 July 2013.
[19] Wangchai, S., Hastie, D.B. and Wypych, P.W. The investigation of particle flow mechanisms of bulk materials in dustiness testers, Particulate Science and Technology, Vol. 34(2), 2016, pp. 241-254.
[20] Yang, R.Y., Zou, R.P. and Yu, A.B. Microdynamic analysis of particle flow in a horizontal rotating drum, Powder Technology, Vol. 130(1-3), 2003, pp. 138-146.